ELECTRICALLY INDUCED DYNAMICS OF COLLOIDAL PARTICLES DISPERSED IN NEMATIC LIQUID CRYSTAL

O.P. PISHNYAK, S. TANG, J.R. KELLY, S.V. SHIYANOVSKII, O.D. LAVRENTOVICH

Liquid Crystal Institute and Chemical Physics Interdisciplinary Program, Kent State University
(Kent, OH 44242, USA)

UDC 532.783, 532.582.7, 538.956

We study the behavior of colloidal particles dispersed in a nematic liquid crystal. Particles create defects of a dipolar type (hyperbolic hedgehogs) in the otherwise homogeneous director field due to the normal anchoring of the nematic director at the particle's surface. Being heavier than the surrounding nematic, the particles still do not fall at the bottom of the cell, and levitate in the nematic bulk thanks to the elastic repulsion from the bounding plates mediated by director distortions [1]. Contrary to an intuitive expectation, the larger the particles, the further away they are repelled from the bottom of the cell. By applying the electric field perpendicular to the overall director, one lifts the particles either to the top of the cell or to the bottom. The direction of this lift depends on the polarity of the director dipole; we discuss the elastic and dielectrophoretic forces among the possible mechanisms of the lift. By switching the electric field on and off, one creates a material flow (backflow effect) that carries particles in two antiparallel directions in the plane of the cell. The velocity of particles can be controlled by the amplitude and duty ratio of the modulated waveform. Numerical simulations of the backflow agree well with the experimental observations, suggesting that the bidirectional dynamics of colloidal particles is controlled mostly by the backflow.

1. Introduction

Colloidal systems represent an old but still very active research topic. Recently, the field has been enriched by the introduction of liquid crystalline colloids, i.e., colloidal systems in which the dispersive medium is a liquid crystal (LC). In addition to the well-known interparticle forces, such as electrostatic and van der Waals forces, and the entropy (excluded volume) effects, LC colloids demonstrate fascinating elasticity-mediated interactions [2]. Typically, anisotropic molecular interactions set a preferred molecular orientation of the LC director at the colloid-LC interface. Since the interface is curved (say, spherical, as in this work), the surface anchoring creates director distortions in the bulk that strongly contribute to interparticle interactions [3,4]. The underlying physics is based on the unusual features of the elastic free energy and the surface energy density of LC. A particle of a typical radius R embedded in the nematic matrix is associated with the energy of director distortions that scales as KR and the surface anchoring energy that scales as WR^2. Here K is the Frank elastic constant of director distortions and W is the (polar) anchoring energy, i.e. the work needed to reorient the director away from the preferred (set, for example, by rubbing) direction by 90 degrees (calculated per unit area). Clearly, if the particle is larger than some critical radius $R_c \sim K/W$, it will create director distortions in the surrounding LC. When the preferred orientation of the director is along a normal to the particle/LC interface (this case we consider in the article), then the particle creates a defect of a dipolar type, Fig. 1. A small particle, $R \ll K/W$, would not distort the director field much.

The case of $R \gg K/W$ represents the most dramatic departure of the LC colloids from their isotropic counterparts, as the elastic interactions bring a decisive long-range contribution to the interparticle interactions [2]. The elasticity-mediated forces cause fascinating phenomena such as the ordering of colloidal particles into chains [2] and hexagonal lattices [5]; attraction of colloids to defects in the director field [6], trapping of

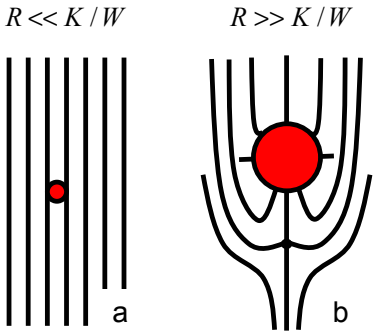

Fig. 1. Schematic of a colloidal particle in LC. (*a*) Small particle does not disturb the LC director. (*b*) Particle with the size larger than some critical radius $R_c \sim K/W$ creates a satellite defect, a hyperbolic hedgehog; note the dipolar symmetry of the overall director distortion around the particle

the particles at the LC-isotropic interface [7], repulsion of a colloid from the bounding wall [1], *etc.*

Since LCs are anisotropic dielectrics and anisotropic (weak) conductors, it is natural to expect that the LC colloids should also exhibit a number of interesting field-induced effects. Recent studies demonstrated that the electric field can cause the translational and orientational motions of colloids in the LC medium [8–11]. The reorientation of LC molecules by an external field leads to a backflow, which was nicely visualized by Zou and Clark [12], opening the possibility for the particles manipulation [11]. This may result in many practical applications, including particles sorting, electrically-driven LC microfluidic devices, development of electrophoretic displays, *etc.*

The central question in the rapidly growing field of LC colloids is the role of the director distortions, especially in the dynamic phenomena. In this paper, we extend our preliminary studies [1] of the dynamics of colloidal particles caused by the electric field in a homogeneously aligned LC cell. First, we quantify the elastic repulsion between a heavy colloidal particle and the bounding wall of LC. Interestingly, the elastic "buoyant" force, which keeps the particle in the nematic bulk, grows with the particle size as R^4; i.e., faster than the gravity force R^3. As a result, a larger particle finds itself farther away from the bottom of the cell as compared to a smaller particle. Second, we discuss the lifting forces that move the particles toward the bounding plates in the presence of the electric field. Here, two mechanisms are possible: an elastic entrapment similar to the one described in [6] and dielectrophoresis (or Kelvin forces) discussed in [13–15]. Finally, we analyze the backflow-induced bidirectional motion of particles. We use the fluorescence confocal polarization microscopy (FCPM) [16] to determine the director orientation around particles and to trace their location and dynamics. The velocity of particles agrees well with the idea of that their dynamics is controlled by the backflow effect.

The article is organized as follows. Section 2 describes the experimental set-up. Section 3 quantifies the elastic interaction of a particle with the bounding walls. Section 4 discusses the lifting forces of the elastic and dielectric nature. Section 5 describes the backflow effects.

2. Experiment

We studied the mixtures of nematic LC E7 (Merck) with small concentrations of colloidal particles (<1% by weight). The surface of particles was modified by *octadecyltrichlorosilane* (Sigma-Aldrich) to promote normal boundary conditions of director **n** at particle's surface. To modify the surface, we dispersed some quantity of colloidal spheres in the same amount of mixture hexane/octadecyltrichlorosilane (1% wt.). After the heating and evaporating of hexane, 4.9 and 9.6 μm in diameter glass particles (Duke Scientific) were dispersed in E7 doped with a small amount (0.01 wt. %) of fluorescent dye N,N'-Bis(2,5-di-tert-butylphenyl)-3,4,9,10-perylenedicarboximide (BTBP, Sigma-Aldrich). We filled the cells formed by glass substrates covered with ITO and rubbed polyimide PI2555 (Microsystems) layers with the obtained mixture. The rubbing results in a small (1–2°) pretilt angle of the director.

Both polarization microscopy (PM) and FCPM studies revealed the formation of hyperbolic hedgehogs accompanying each colloidal particles (Fig. 2) and thus confirming the normal director orientation at the particle's surface. When there is no electric field, the colloidal particles are levitating in the bulk (Fig. 2,*k–n*). Interestingly, the heavier 9.6-μm particles are located closer to the middle of the cell than the smaller 4.9-μm particles.

The applied electric field, directed vertically along the axis z in Fig. 2, reorients the director, and the particles move toward the substrates (Fig. 2,*o–r*). The particles with the opposite orientation of the elastic dipole (determined by the location of hyperbolic hedgehogs) move to the opposite substrates.

The spatial separation of particles according to the orientation of their elastic dipoles toward the top and bottom substrates offers an opportunity to move these particles along two opposite directions in the plane of the cell, by using the phenomenon of backflow, i.e., a material flow caused by the director reorientation in the applied electric field. The symmetry of a planar cell dictates that the backflow velocity is zero in the middle of the cell but reaches its maximum near the top and bottom plates; the directions of the mass flow near the top and the bottom plates are opposite to each other. This antisymmetric backflow can be controlled by changing the frequency and the modulation profile of an applied field [17]. Thus, the bidirectional translation of particles can be controlled [1].

3. Particle-Wall Interaction

In the absence of a field, colloidal particles accompanied by defects of a dipolar type are floating in the bulk balanced by repulsive forces of the dipole-dipole interaction, whose potential can be written as [2]

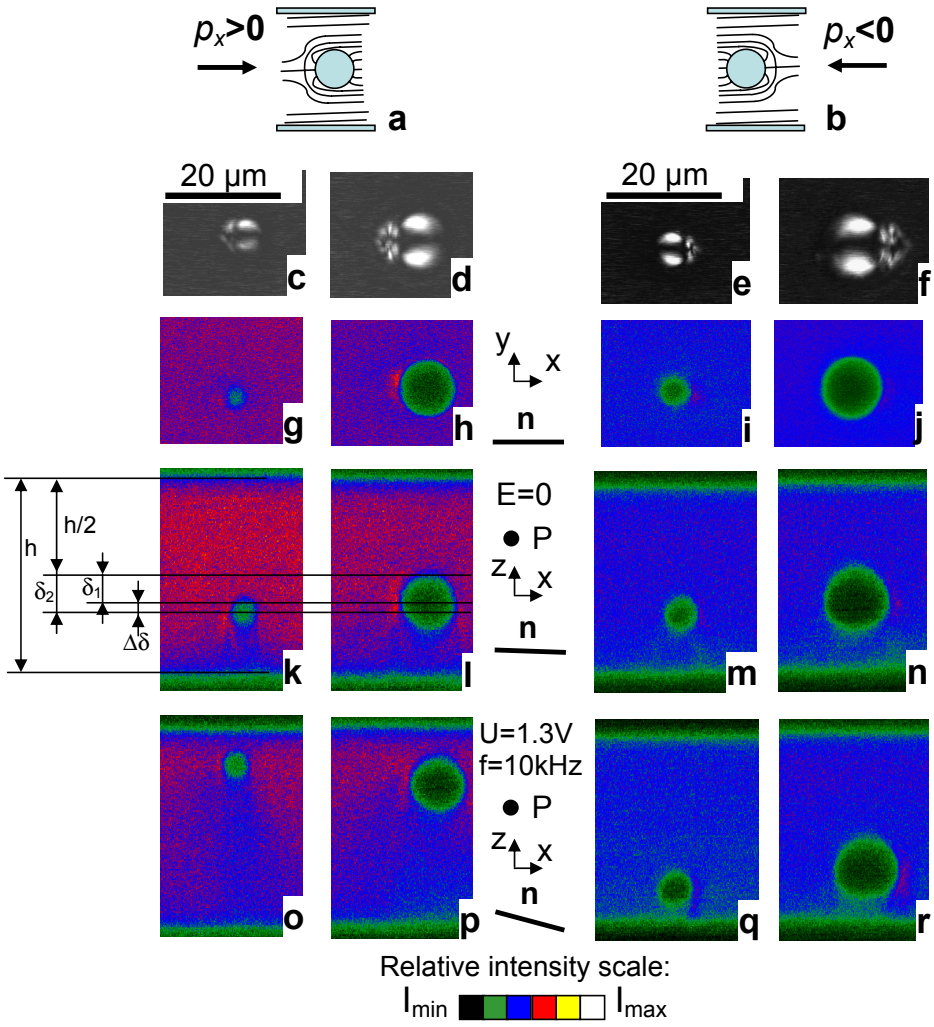

Fig. 2. FCPM studies of the director structure around glass spherical particles (4.9 and 9.6 μm in diameter) with normal boundary conditions in a $h \approx 33$ μm planar cell. (*a*, *b*) Scheme of the director distribution around particles; hyperbolic hedgehogs with different orientations are observed: left-oriented hedgehogs (left column) and right-oriented hedgehogs (right column). The orientations of polarizer P, director $\mathbf{n}$, and coordinate axes are shown. (*c*-*f*) Transmission mode, crossed polarizers. (*g*-*j*) Fluorescent mode, scan in the xy plane. (*k*-*n*) Fluorescent mode, scan in the z-direction. No field is applied; particles are levitating in the bulk. Distances from big (δ_1) and small (δ_2) particles to the middle of the cells are shown. The bigger particle is located closer to the middle than the small one ($\Delta\delta = \delta_2 - \delta_1 \sim 2$ μm). (*o*-*r*) Fluorescent mode, scan in the z-direction. Electric field ($U = 1.3$ V, $f_c = 10$ kHz) is applied. Particles with opposite orientations of hyperbolic hedgehogs are pushed to the opposite substrates

$E = 4\pi K p^2 \frac{1-3\cos^2\phi}{r^3}$, and the gravitational force $F_g = \frac{4}{3}\pi R^3 (\rho_p - \rho) g$. Here, $K \approx 15pN$ is the average of splay $K_1 = 11.7pN$ and bend $K_3 = 19.5pN$ constants of E7 [18]; $p = AR^2$, $A = 2.04$ is the numerical constant [2]; R is the particle's radius; r is the distance between two parallel dipoles, ϕ is the angle between the dipole's axis and the line joining the centers of dipoles (for our geometry, $\cos\phi \approx 0$); $\rho_p \approx 2.5$ g/cm^3 (Duke Scientific) and $\rho \approx 0.98$ g/cm^3 (Merck) are the densities of particles and E7, respectively; $g \approx 9.8$ m/s^2 is the standard gravity. The balance of forces acting on a particle can be written as follows:

$$F = F_0 - F_h - F_g = \frac{3}{2}\pi K A^2 \left(\frac{2R}{h-2\delta}\right)^4 -$$

$$-\frac{3}{2}\pi K A^2 \left(\frac{2R}{h+2\delta}\right)^4 - \frac{4}{3}\pi R^3 (\rho_p - \rho) g = 0, \qquad (1)$$

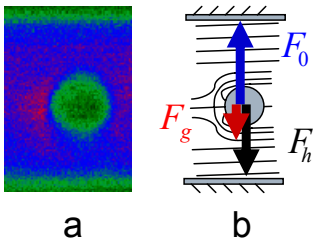

Fig. 3. (*a*) FCPM image of a $2R = 4.9$ μm glass particle floating in the LC bulk and accompanied by a satellite defect. (*b*) Sketch of the director distribution and forces (gravitational F_g and repulsion ones F_0, F_h) acting on the particle

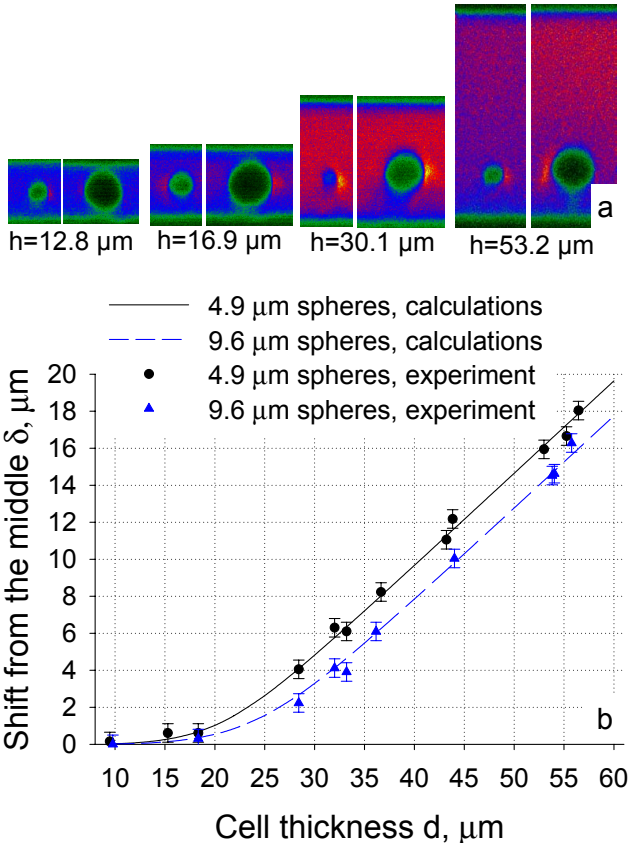

Fig. 4. (*a*) FCPM images of glass particles in LC cells with different thicknesses. The thicker the cell, the closer the particles are to the bottom substrate. Note that bigger particles are closer to the middle of the cell than smaller ones. (*b*) Plot demonstrating the experimental and calculated [according to Eq.(1)] shift δ of the $2R = 4.9$ μm and $2R = 9.6$ μm glass particles dispersed in E7 from the middle of the cell

where F_0 and F_h are the repulsion forces between the dipole and its mirror images with respect to the bottom $z = 0$ and top $z = h$ plates, respectively (Fig. 3), h is the cell thickness, δ is the shift of the particle's center from the middle of the cell $z = h/2$, and R is the particle's radius ($2R = 4.9$ and 9.6 μm). The position of particles in the LC bulk can be determined from the FCPM scans of cells with different thicknesses, Fig. 4,*a*. The experimental error related to aberrations of the light propagating in the birefringent media can be mitigated by a) knowing the thickness of the cell; b) knowing the scan distance along the z-axis; c) knowing the size of particles. The calculated [according to Eq.(1)] and experimental dependences of δ are shown in Fig. 4,*b*. $\delta < 1$ μm if $h < 20$ μm for both particles and monotonously grows with increase in the thickness. Note that larger (and heavier) particles are closer to the middle of the cell than smaller ones, which is rather counterintuitive.

4. Effect of Lifting Forces

When the voltage exceeds the Friedericksz threshold $U_{\rm th} = \pi\sqrt{\frac{K_1}{\varepsilon_0\Delta\varepsilon}} \approx 0.92$ V [17], the LC director is reoriented, and the particles move toward the substrates. Here, $\varepsilon_0 \approx 8.85 \times 10^{-12}$ C^2/N $\cdot$ m^2 is the permittivity of free space, $\Delta\varepsilon = \varepsilon_{||} - \varepsilon_{\perp} = 19.0 - 5.2 = 13.8$ (Merck) is the dielectric anisotropy of E7. The increase rate of the voltage envelope was set low, 0.1 V/s, to minimize the backflow, but the carrier frequency was high, $f_c = 10$ kHz (to avoid electrohydrodynamics caused by ions). The pretilt angle and the orientation of a hedgehog determine the direction of the upward or downward shift of the particles, Fig. 2,*o–r*.

There are two possible mechanisms that cause a shift of the colloids from the middle of the cell toward the top and bottom plates. The first one is the elastic mechanism [6] associated with the elastic interactions of the director around the colloid and near the surfaces. The second mechanism is of the dielectrophoretic origin [13–15]: as the electric field and the dielectric permittivity in a distorted cell change along the vertical z-axis, the dielectric sphere might experience a force resolved along the z-axis. Below, we estimate the typical forces associated with each mechanism.

Director distortions near the substrates concentrate over the length $\xi = \frac{h}{U}\sqrt{\frac{K}{\varepsilon_0\Delta\varepsilon}}$. The elastic energy gained by moving a spherical particle from the uniform middle of the cell toward the distorted regions near the substrates can be estimated as $\Delta E \sim KR^3/\xi^2$ [6]. The corresponding trapping force $F_{\rm trap} \sim KR^3/\xi^3 \sim 1.2 - 9.4pN$ is rather significant, as compared to the gravity forces and elastic repulsive forces; e.g., Eq. (1) yields

$F_h \approx 0.05 - 1.2pN$, $F_0 \approx 0.7 - 6.2pN$ for $h = 33$ μm, and $2R = 5 - 10$ μm.

The dielectrophoretic effect is associated with different director orientations near the substrates and the middle of a cell. The electric field is a function of the z-coordinate; the dependence can be found from the condition of the constancy of the electric displacement as

$$E(z) = \frac{E_0 \varepsilon_{\text{eff}}}{\varepsilon_\perp \sin^2\theta + \varepsilon_\parallel \cos^2\theta},$$

where θ is the angle between the applied field $\mathbf{E}_0 = \mathbf{e}_z U/h$ and the local director, and $\varepsilon_{\text{eff}} = h \Big/ \int_0^h \left(\varepsilon_\perp \sin^2\theta + \varepsilon_\parallel \cos^2\theta\right)^{-1} dz$. For simplicity, we assume that the director in the middle of the cell is completely reoriented along the field, so that $\theta = 0$, while it remains parallel to the substrates near the substrates, $\theta = 90°$. In this case, the values of the electric field at the center of cell and near the substrates (say, the top substrate) are $E^{\text{center}} = E_0 \varepsilon_{\text{eff}}/\varepsilon_{||}$ and $E^{\text{top}} = E_0 \varepsilon_{\text{eff}}/\varepsilon_\perp$, respectively.

A dielectric sphere with permittivity different from that of the matrix might experience a force in a non-uniform electric field. To roughly estimate this force, we first recall that the polarization of a dielectric sphere of radius R placed in a uniform electric field $\mathbf{E}_0$ is

$$\mathbf{P} = 4\pi R^3 \varepsilon_0 \frac{\varepsilon_p - \varepsilon_{LC}}{\varepsilon_p + 2\varepsilon_{LC}} \mathbf{E}_0$$

[13], where ε_p and ε_{LC} are dielectric constants of the particle and LC, respectively. The energy of the particle in the uniform field is $W = -\frac{1}{2}\mathbf{P}\mathbf{E}_0$. When the particle is transferred from the middle of the cell toward the substrate, the associated energy difference is roughly

$$\delta W = W^{\text{center}} - W^{\text{top}} =$$

$$= -2\pi R^3 \varepsilon_0 E_0^2 \left[\left(\frac{\varepsilon_p - \varepsilon_\parallel}{\varepsilon_p + 2\varepsilon_\parallel} \right) \frac{\varepsilon_{\text{eff}}^2}{\varepsilon_\parallel^2} - \left(\frac{\varepsilon_p - \varepsilon_\perp}{\varepsilon_p + 2\varepsilon_\perp} \right) \frac{\varepsilon_{\text{eff}}^2}{\varepsilon_\perp^2} \right],$$

and the corresponding dielectrophoretic force can be estimated as $F_{\text{diel}} \sim -\delta W/\xi$. With $\varepsilon_p = 5.8$ (Duke Scientific), $h = 33$ μm, $U = 1.3$ V, and $\varepsilon_{\text{eff}} \approx 8$ (low field regime), we find that the net force is $F_{\text{diel}} \sim 0.2pN$ for $2R = 5$ μm and $F_{\text{diel}} \sim 1.9pN$ for $2R = 10$ μm. The force is directed from the middle of the cell toward the substrate. It appears that in the low-field regime $E < 0.06$ V/μm, the dielectrophoretic force is weaker than the elastic trapping force near the substrates, so the prime mechanism for particle's lifting in this case is the elastic one; however, for higher fields, the dielectrophoretic force becomes quickly dominating: for $E \sim 0.5$ V/μm, one finds $F_{\text{diel}} \sim 2500pN$ at $2R = 5$ μm and $F_{\text{diel}} \sim 20000pN$ at $2R = 10$ μm. The separation of the elastic and dielectrophoretic mechanisms deserves further studies.

Because of the specific antisymmetric character of the backflow in a LC cell with "antiparallel" boundary conditions at the opposite plates, the particles' shift toward the top and bottom substrates allows one to establish a bidirectional flow that would carry particles with different orientations of the elastic dipole along two antiparallel directions [1]. Below, we discuss the phenomenon in more details.

5. Calculations of the Backflow

In this section, we discuss the director reorientation dynamics and the backflow in a regular homogeneously aligned LC cell with a small pretilt angle 2° of the director. We studied mixtures of E7 with $2R \approx 4.9$ μm silica particles (Bangs Laboratories, Inc.) filled into $h = 21$ μm planar cells. We created the backflow by applying a voltage $U = 10$ V, $f_c = 10$ kHz (generator DS345, Stanford Research Systems, Inc.), modulated with the frequency $f_m = (0.5 - 100)$ Hz (following the lift-creating pulse described above), Fig. 5,a. The duty ratio defined as the duration of the field ON to the total duration of the field cycle was 50%.

The modeling of backflow is based on the Ericksen–Leslie (EL) equations [19–22] of nematodynamics. These equations couple the director reorientation with the hydrodynamic flow of a LC fluid. We assume that the director $\mathbf{n} = \{\cos\theta(z,t), 0, \sin\theta(z,t)\}$ is in the xz plane, and that the hydrodynamic flow has only the x component, $\mathbf{v} = \{v(z,t), 0, 0\}$. We neglect the flow inertia term, because the flow relaxation time $\tau_v \approx \rho h^2/\pi^2\alpha_4 \sim 1$ μs is much shorter than the director relaxation times $\tau_{\text{on}} \approx (\alpha_3 - \alpha_2)\, h^2/\varepsilon_0 \left(\varepsilon_\parallel - \varepsilon_\perp\right) U^2 \sim 10$ ms and $\tau_{\text{off}} \approx (\alpha_3 - \alpha_2)\, h^2/\pi^2 K_1 \sim 1$ s, and write the EL equations as

$$(\alpha_3 - \alpha_2)\,\dot{\theta} = -G_\theta - \left(\alpha_3 \cos^2\theta - \alpha_1 \sin^2\theta\right) v', \qquad (2)$$

$$\left(\alpha_3 \cos^2\theta - \alpha_2 \sin^2\theta\right)\dot{\theta} + \tilde{\alpha}\,(\theta)\, v' = \sigma_{zx}(t), \qquad (3)$$

where the dot and prime denote the time and z-derivatives, respectively; $\tilde{\alpha}(\theta) = \frac{1}{2}\Big[\frac{1}{2}\alpha_1 \sin^2 2\theta + (\alpha_5 - \alpha_2)\sin^2\theta + \alpha_4 + (\alpha_3 + \alpha_6)\cos^2\theta\Big]$; G_θ is the variational

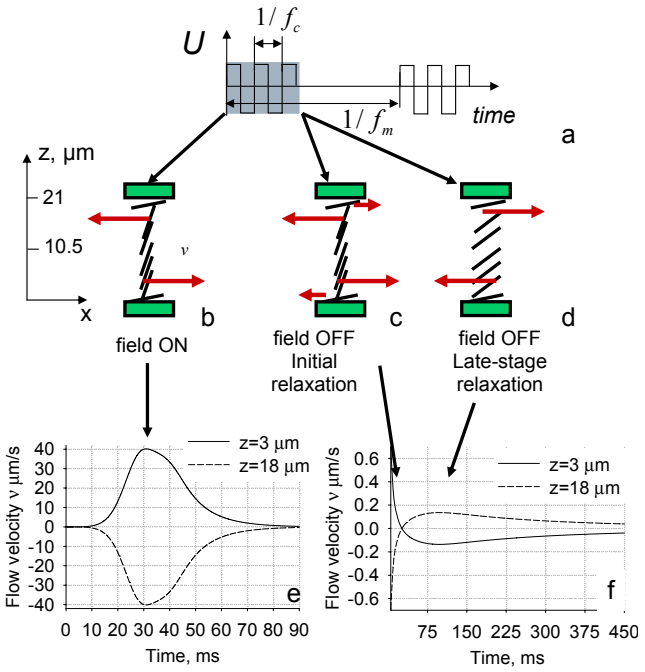

Fig. 5. Dynamics of the director reorientation and the backflow. (*a*) Scheme of the applied modulated signal. (*b-d*) Sketch of the director reorientation when the field is turned ON and OFF. (*e,f*) Calculated backflow in a planar cell. When the field is turned ON, the director reorientation causes a direct flow $v_{\rm on}\,(h/2 < z < h) < 0$, $v_{\rm on}\,(0 < z < h/2) > 0$, which vanishes with time (*e*). When the field is turned OFF, the director relaxation near the surfaces causes a direct flow $v_{on}\,(h/2 < z < h) < 0$, $v_{\rm on}\,(0 < z < h/2) > 0$ initially. With time, the director relaxation in the bulk causes a reverse flow $v_{\rm on}\,(h/2 < z < h) > 0$, $v_{\rm on}\,(0 < z < h/2) < 0$ (f)

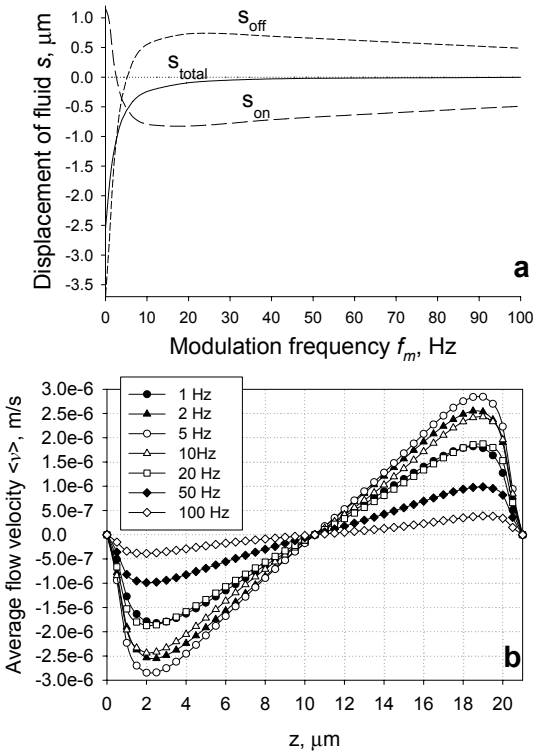

Fig. 6. (*a*) Simulated displacement following the switch ON ($s_{\rm on}$), switch OFF ($s_{\rm off}$), and during the entire cycle, ON+OFF ($s_{\rm total}$), for $z = 2$ μm. (*b*) The calculated average flow velocity profile observed under a modulated signal for different modulation frequencies f_m

derivative of the Frank–Oseen energy,

$$G_\theta = -\left(K_3 \sin^2\theta + K_1 \cos^2\theta\right)\theta'' - \frac{1}{2}\left(K_3 - K_1\right) \times$$

$$\times \sin 2\theta\theta'^2 - \frac{1}{2}\varepsilon_0\left(\varepsilon_\parallel - \varepsilon_\perp\right) U^2 \sin 2\theta \left[I_1 \tilde{\varepsilon}\left(\theta\right)\right]^{-2}, \qquad (4)$$

with $I_1 = \int\limits_0^d dz/\tilde{\varepsilon}\left(\theta\right)$, $\tilde{\varepsilon}\left(\theta\right) = \varepsilon_\parallel \sin^2\theta + \varepsilon_\perp \cos^2\theta$; $\sigma_{zx}(t)$ is the zx-component of the nematic strain tensor that does not depend on z and is determined from the boundary condition $v\left(z=0\right) = v\left(z=h\right) = 0$;$\alpha_1 = -21$, $\alpha_2 = -282$, $\alpha_3 = -1$, $\alpha_4 = 225$, $\alpha_5 = 92$, $\alpha_6 = -191$ (all in mPa $\cdot$ s units) are the viscosity coefficients [18]. We solve Eqs. (2) and (3), by using the implicit Crank–Nicolson scheme for time derivatives [23].

The flow behavior is different for $f_m \ll \tau^{-1} = \left(\tau_{\rm on} + \tau_{\rm off}\right)^{-1} \approx \tau_{\rm off}^{-1} \approx 1$ Hz, when $\mathbf{n}$ has time to equilibrate, and for $f_m \geq \tau^{-1}$, when $\mathbf{n}$ does not equilibrate. The regime $f_m \ll \tau^{-1}$ is well studied [17]. When the field is switched ON, a counterclockwise rotation of $\mathbf{n}$ causes a flow with $v_{\rm on}\,(h/2 < z < h) < 0$ and $v_{\rm on}\,(0 < z < h/2) > 0$, Fig. 5,*b,e*. With time, this flow gradually vanishes. The symmetry $\theta\left(z\right) = \theta\left(h - z\right)$ and $v\left(z\right) = -v\left(h - z\right)$ allows us to discuss the bottom half only. The flow-produced displacement $s_{\rm on}\,(0 < z < h/2) > 0$ of fluid is maximum, $s_{\rm on} \approx 1.2$ μm, at $z \approx 2$ μm. When the field is switched OFF, the elastic torque causes a clockwise rotation of the director near the substrates and initially $v_{\rm on}\,(h/2 < z < h) < 0$, $v_{\rm on}\,(0 < z < h/2) > 0$. With time, the director relaxation in the bulk causes a slow reverse flow so $v_{\rm on}\,(h/2 < z < h) > 0$, $v_{\rm on}\,(0 < z < h/2) < 0$ now, Fig. 5,*c,d,f*. When the field is switched OFF, the fluid displacement is larger and of opposite sign, $s_{\rm off} \approx -3.7$ μm for $z \approx 2$ μm. The total displacement per one cycle is negative, $s_{\rm total} = s_{\rm on} + s_{\rm off} \approx -2.5$ μm, Fig. 6,*a*.

When $f_m \geq \tau^{-1}$, the equilibration after each ON and OFF switch is not complete, and the pictures are very different. Both $s_{\rm on}$ and $s_{\rm off}$ initially become shorter and then switch signs, but their sum $s_{\rm total} = s_{\rm on} + s_{\rm off}$ remains negative, Fig 6,*a*. The time average of the backflow for different modulation frequencies f_m can be calculated as follows:

$$\langle v(z) \rangle = \frac{\int_{1/f_m} v(z,t)\, dt}{1/f_m}. \qquad (5)$$

The results of calculations are in Fig. 6,*b*. The particles are thus carried bidirectionally: those near the top move toward $+x$, and those near the bottom move toward $-x$; in both cases, the hedgehog leads the way, Fig. 7,*a–c*. The motion is similar to one observed in [10] with the difference that, in our case, it is bidirectional rather than unidirectional. For a low f_m, the average velocity of the fluid $\langle v \rangle = s_{\rm total} f_m$ increases linearly with f_m. In the limit $f_m \to \infty$, small back and forth reorientations cancel each other so that $\langle v \rangle \to 0$. The dependence $\langle v \rangle (f_m)$ is nonmonotonous with $\langle v \rangle \to 0$ for low and high f_m's and a maximum for an intermediate f_m. From Fig. 6,*b*, it is clearly seen that the maximum flow velocity $\langle v \rangle \sim 2 - 3$ μm/s is observed at $f_m \sim 2 - 10$ Hz. This is exactly what we observed in the experiment for $\langle v_p \rangle (f_m)$, Fig. 7,*d*. The good agreement suggests that the prime mechanism of the particle migration in our experiments is the backflow effect.

6. Conclusions

We have presented the experimental results on the static and dynamics of colloidal particles dispersed in a nematic LC. The particles are big enough (microns) to cause dipole-like elastic distortions of the director around them. In the absence of the electric field, the particles levitate in the bulk of the cell, as the gravity forces are opposed by repulsive forces between the particle and the bounding walls. By measuring the position of a levitating particle as a function of the thickness of the cell, we determine the elastic repulsive force between the particle and the rigid wall and find it to agree well with the predictions of the elastic theory by Poulin *et al.* [2].

In the absence of the electric field, the elastic dipole is roughly horizontal and oriented along the direction of rubbing in the cell, in any of the two available directions. When the field is applied, this symmetry is broken, and the particles with opposite directions of the elastic dipole

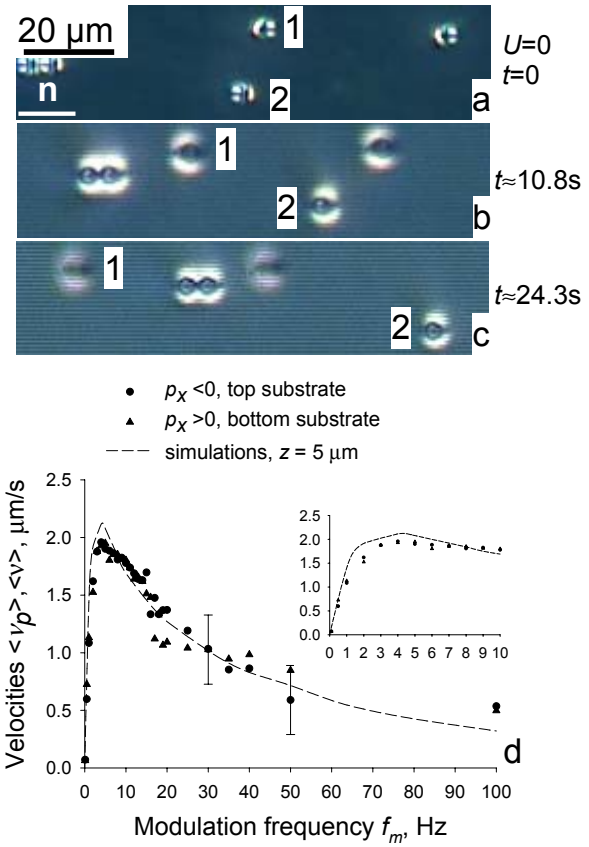

Fig. 7. Electric-field induced bidirectional motion of silica particles (4.1 μm in diameter, Bangs Laboratories, Inc.) *1* and *2* accompanied by oppositely oriented hyperbolic hedgehogs in a 21-μm planar cell. (*b*) initial state, no field applied; (*c, d*) bidirectional motion of the particles driven by a modulated electric signal with $U = 10$ V, $f_c = 10$ kHz, $f_m = 10$ Hz. (*d*) Average particle velocity $\langle v_p \rangle$ vs. f_m for $f_c = 10$ kHz. The line shows the simulated average backflow velocity $\langle v \rangle (f_m)$, at $z = 5$ μm. The inset shows the enlarged plot for $0 < f_m \leq 10$

move to opposite substrates. We discuss two possible mechanisms behind this effect, elastic trapping and dielectrophoretic effect. The elastic forces prevail at low fields (0.1 V/micron or less) while the dielectrophoretic forces are expected to dominate at higher fields.

The most dramatic effect of the applied electric field on colloidal particles is through the backflow effect. The latter causes the particles to move along the bounding plates. Since the backflow is antisymmetric, the particles with opposite polarities of the elastic dipole are moving into opposite directions. The results of numerical simulations of the backflow profile are in a good agreement with the experimental data on the velocities of particles.

To conclude, the experiments demonstrate that the particle's dynamics is controlled by director distortions, which can be controlled, in turn, by the external fields. Thus, the colloidal dynamics in LCs demonstrates a rich variety of mechanisms and effects involved. Some of them are not explored yet. For example, by reducing the thickness of a cell or increasing the diameter of particles, one can strongly enhance their scattering by one another and thus study the phenomena such as jamming [24]; these studies are currently in progress.

We acknowledge the useful discussions with A. Jakli, V. Nazarenko, and support by NSF DMR grant 0504516, DOE grant DE-FG02-06ER 46331 and Samsung Electronics Corp.

1. O.P. Pishnyak, S. Tang, J.R. Kelly, S.V. Shiyanovskii, and O.D. Lavrentovich, Phys. Rev. Let. **99**, 127802 (2007).
2. P. Poulin, H. Stark, T.C. Lubensky, and D.A. Weitz, Science **275**, 1770 (1997).
3. P.G. de Gennes, J. Prost, *The Physics of Liquid Crystals*, (Clarendon Press, Oxford, 1993).
4. M. Kleman, O.D. Lavrentovich, *Soft Matter Physics: An Introduction*, (Springer, New York, 2003).
5. I.I. Smalyukh, S. Chernyshuk, B.I. Lev, A.B. Nych, U. Ognysta, V.G. Nazarenko, and O.D. Lavrentovich, Phys. Rev. Lett. **93**, 117801 (2004).
6. D. Voloschenko, O.P. Pishnyak, S.V. Shiyanovskii, and O.D. Lavrentovich, Phys. Rev. E **65**, 060701 (2002).
7. J. West, A. Glushchenko, G. Liao, Y. Reznikov, D. Andrienko, and M. Allen, Phys. Rev. E **66**, 012702/1-4 (2002).
8. T. Togo, K. Nakayama, M. Ozaki, and K. Yoshino, Jpn. J. Appl. Phys. **36**, L1520 (1997).
9. G. Liao, I.I. Smalyukh, J.R. Kelly, O.D. Lavrentovich, and A. Jakli, Phys. Rev. E **72**, 031704/1-5 (2005).
10. I. Dierking, G. Biddulph, and K. Matthews, Phys. Rev. E **73**, 011702/1-6 (2006).
11. Yositaka Mieda and Katsushi Firutani, Appl. Phys. Lett. **86**, 101901/1-3 (2005).
12. Zhong Zou and Noel Clark, Phys. Rev. Lett. **75**, 1799, (1995).
13. J.D. Jackson, *Classical Electrodynamics*, 3^{rd} ed., (Academic Press, New York, 1998).
14. N. Gheorhiu, J.L. West, A.V. Glushchenko, and M. Mitrokhin, Appl. Phys. Lett. **88**, 263511 (2006).
15. H. Ren, S.-T. Wu, and Y.-H. Lin, Phys. Rev. Let. **100**, 117801 (2008).
16. I.I. Smalyukh, S.V. Shiyanovskii, and O.D. Lavrentovich, Chem. Phys. Lett. **336**, 88-96 (2001).
17. L.M. Blinov, V.G. Chigrinov, *Electrooptic Effects in Liquid Crystal Materials* (Springer, New York, 1994).
18. H. Wang, T.X. Wu, S. Gauza, J.R. Wu, and S.-T. Wu, Liq. Cryst. **33**, 91–98 (2006).
19. F.M. Leslie, Quart. J. Mech. Appl. Mah. **19**, 357 (1966).
20. F.M. Leslie, Arch. Ration. Mech. Analysis **28**, 265 (1968).
21. J.L. Ericksen, Trans. Soc. Rheol. **5**, 23 (1961).
22. J.L. Ericksen, Mol. Cryst. Liq. Cryst. **7**, 153 (1969).
23. J. Crank and P. Nicolson, Proc. Camb. Phil. Soc. **43**, 50 (1947).
24. I.T. Georgiev, B. Schmittmann, and R.K.P. Zia, Phys. Rev. Lett. **94**, 115701 (2005).

ЕЛЕКТРИЧНО ІНДУКОВАНА ДИНАМІКА КОЛОЇДНИХ ЧАСТИНОК, ДИСПЕРГОВАНИХ В НЕМАТИЧНОМУ РІДКОМУ КРИСТАЛІ

О.П. Пишняк, С. Танг, Дж.Р. Келлі, С.В. Шияновський, О.Д. Лаврентович

Р е з ю м е

В статті розглянуто поведінку колоїдних частинок в нематичному рідкому кристалі. В однорідному полі директора навколо частинок виникають дефекти дипольного типу (гіперболічний їжак) завдяки нормальним межовим умовам директора на поверхні частинок. Незважаючи на те, що частинки важче оточуючого нематика, частинки не опускаються на дно комірки, а левітують в об'ємі нематика завдяки еластичним силам відштовхування від підкладок комірки, спричинених деформаціями директора. Всупереч інтуїтивним очікуванням, більші за розміром частинки знаходяться далі від нижньої підкладки завдяки більшим силам відштовхування. Після прикладання електричного поля перпендикулярно до директора частинки рухаються до поверхонь верхньої або нижньої підкладки. Напрямок сили підйому залежить від полярності диполя; серед імовірних механізмів ми розглядаємо еластичні та діелектрофоретичні сили. Періодично включаючи та виключаючи електричне поле, можливо створити потік речовини (ефект зворотнього потоку), який буде переносити частинки в двох протилежних напрямках в площині комірки. Швидкість частинок може контролюватися амплітудою і періодом модуляції електричного сигналу. Числові розрахунки зворотнього потоку добре співвідносяться з експериментальними вимірами, підтверджуючи, що двонапрямлений рух колоїдних частинок спричинений, головним чином, зворотнім потоком.